

## Piezoelectric response around ferroelectric domain walls in crystals with engineered domain configuration

Haiyan Guo, Alexei A. Bokov, and Zuo-Guang Ye\*

*Department of Chemistry and 4D LABS, Simon Fraser University, Burnaby, British Columbia, Canada V5A 1S6*

(Received 9 January 2009; revised manuscript received 3 January 2010; published 28 January 2010)

We report investigation of the piezoelectric response on a nanoscale in poled ferroelectric crystals with engineered domain configuration. Piezoresponse force microscopy of the (111) surface of a ( $\langle 111 \rangle$ -poled) tetragonal  $0.63\text{Pb}(\text{Mg}_{1/3}\text{Nb}_{2/3})\text{O}_3$ - $0.37\text{PbTiO}_3$  piezoelectric/ferroelectric crystal revealed that the piezoelectric coefficient  $d_{33}$  is significantly reduced within the distance of  $\sim 1 \mu\text{m}$  from the uncharged engineered domain walls. This finding is essential for understanding the mechanisms of the giant piezoresponse in relaxor-based crystals and for designing high-performance piezoelectric materials.

DOI: [10.1103/PhysRevB.81.024114](https://doi.org/10.1103/PhysRevB.81.024114)

PACS number(s): 77.65.-j, 77.80.Dj, 77.84.Ek, 77.84.Cg

### I. INTRODUCTION

The discovery of giant piezoelectricity in relaxor-based ferroelectric single crystals,<sup>1</sup> which demonstrate the piezoelectric coefficients five to ten times as large as in traditional piezoelectric ceramics such as  $\text{Pb}(\text{Zr}_{1-x}\text{Ti}_x)\text{O}_3$  (PZT), makes them the materials of choice for the next generation of electromechanical transducers, sensors, and actuators.<sup>1-4</sup> A great deal of effort has been made to investigate the origin of their extraordinary properties. The polarization rotation model<sup>5,6</sup> attributes the piezoresponse essentially to the intrinsic (crystal lattice strain) effect. However, relaxor-based piezocrystals possess complex polar structure on nanoscopic and microscopic scales, which may include local random fields, specific relaxor polar nanoregions, phase and composition heterogeneities, lamellar nanodomains of adaptive phase, ferroelectric microdomains, etc.<sup>7</sup> These features may in principle play an essential role in piezoelectric response, giving rise to “extrinsic” piezoelectric contributions.<sup>8-13</sup> Experimentally, however, this role has not been clarified. As a result, the mechanisms of high piezoelectricity in relaxor-based ferroelectric crystals remain poorly understood, which forms a serious obstacle for the development of piezoelectric materials.

Significant macroscopic piezoresponse can be observed only in those ferroelectric samples, which have been preliminarily poled by an external electric field to obtain a monodomain state or a state with preferred domain orientation. In many cases (e.g., in ceramics) a monodomain state cannot be attained and the sample consists of multiple domains separated by domain walls.<sup>14</sup> If the applied electric field or mechanical stress forms different angles with the spontaneous polarization vectors of adjacent domains, the wall between them can move and thereby contribute to piezoelectric effect. In conventional ferroelectric ceramic materials this contribution may be of the same order of magnitude as the intrinsic contribution.<sup>15</sup> However, besides the positive effect of enhancing piezoelectric coefficients, domain wall motion can lead to unwanted nonlinearity and hysteresis in the strain-field dependences. In the special case of so-called “engineered domain” configuration in crystals, the walls are arranged in such way that the electric field or stress cannot influence their positions and the corresponding extrinsic pi-

ezoelectric contribution is absent. Surprisingly, the largest piezoelectric coefficients are found right in the crystals with engineered domain configurations, including the relaxor-based perovskite solid solutions.<sup>1-4,16</sup> To explain this fact it is tempting to assume that the regions near the walls possess enhanced piezoelectric properties even though the walls do not move.<sup>17,18</sup> Local measurements of piezoelectric coefficients are needed to verify this hypothesis. However, these measurements cannot be done by conventional methods because of insufficient spatial resolution. To solve this problem, in the present work, we use the technique of piezoresponse force microscopy (PFM), which is expected to be a suitable tool for this purpose because of its proved great capability in visualizing domain walls and measuring piezoelectric properties on the nanoscale.<sup>19</sup> We find that in the vicinity of engineered domain wall the piezoelectric response is significantly reduced, rather than enhanced as has been assumed until now.

### II. EXPERIMENTAL PROCEDURE

Relaxor-based ferroelectric  $(1-x)\text{Pb}(\text{Mg}_{1/3}\text{Nb}_{2/3})\text{O}_3$ - $x\text{PbTiO}_3$  perovskite solid solution crystals grown by the Bridgman method were studied in this work. The crystal of composition  $x=0.37$  (PMN-37PT) having a tetragonal structure (crystal class  $4mm$ ) was chosen for investigation. At this composition the domain size is known to be much larger than in the rhombohedral and monoclinic crystals with smaller PT content ( $x$ ) (Ref. 20) (although the piezoelectric coefficients are not so large) and consequently the piezoresponses from the internal part of the domains and from the near-wall regions can be reliably separated.

Quantitatively the piezoelectric effect can be characterized with the matrix of piezoelectric coefficients,  $d_{ij}$ , through the relation

$$S_j = d_{ij}E_i, \quad (1)$$

where  $E_i$  is a component of the electric field vector and  $S_j$  is a piezoelectric strain component. In ferroelectrics the piezoelectric coefficients are related to the spontaneous polarization vector,  $\mathbf{P}_s$ , through the expression

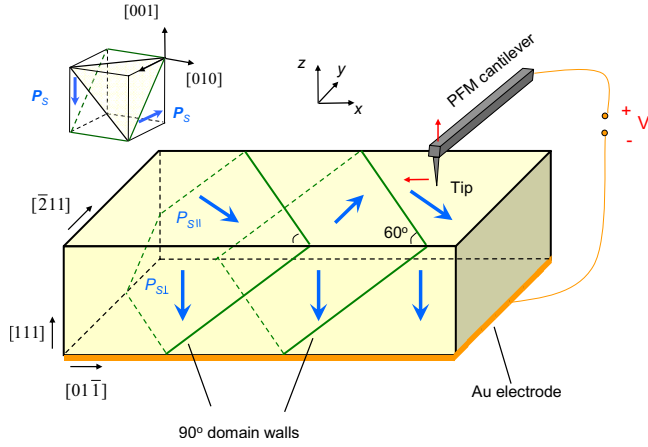


FIG. 1. (Color online) The experimental setup for PFM measurements and schematic diagram of the domain structure in the studied (111)-oriented poled tetragonal PMN-37PT crystal plate (not to scale). Laboratory coordinate system ( $X, Y, Z$ ), crystallographic directions, and the positions of  $90^\circ$  domain walls are indicated. Blue arrows represent the components of spontaneous polarization vector parallel ( $P_{S||}$ ) and perpendicular ( $P_{S\perp}$ ) to the crystal surface in different domains. Red arrows show the vertical and lateral displacements of the PFM tip when the measurement voltage ( $V$ ) is applied. Upper left inset shows the positions of the observed domain wall (outlined by green lines) and crystal surface (represented by the equilateral triangle) with respect to the cubic unit cell of the paraelectric phase.

$$d_{ij} \approx \varepsilon_{im} Q_{jmk} P_{Sk}, \quad (2)$$

where  $\varepsilon_{im}$  and  $Q_{jmk}$  are the dielectric constants and electrostrictive coefficients, respectively.

The PFM experiments were performed on a modified atomic force microscope (Veeco ThermoMicroscopes). The PFM extension included a National Instrument (NI) data acquisition (DAQ) system board, a lock-in amplifier, and a LABVIEW computer controlling system. An ac frequency of 95 kHz was used in the vertical PFM experiments. A 10 kHz ac frequency was used in the lateral PFM measurements in order to avoid possible tip slipping problem at high frequency.<sup>21</sup> The PFM images were developed with the help of WsXM software.<sup>22</sup>

The PFM is a type of scanning probe microscopy,<sup>19</sup> in which the piezoelectric strain is excited by the electric voltage applied between the bottom electrode and the very sharp conducting PFM tip, which touches the crystal surface (see Fig. 1). For technical reasons a high-frequency ac voltage must be used. Movement of the surface related to the piezoelectric strain leads to the displacement of the tip, which can be measured. From these measurements, using Eq. (1), one can estimate the  $d_{ij}$  values (in the laboratory, not the crystallographic, coordinate system) in a small region of the order of a few tens of nanometers. From Eq. (2) the components of  $P_S$  can be estimated. The local  $d_{33}$  coefficient determines the displacement of the tip in the vertical direction, while the  $d_{15}$  coefficient (shear deformations of crystal) is mainly responsible for the lateral displacement in the  $X$  direction (perpendicular to cantilever)<sup>19,23</sup> By scanning the surface point by

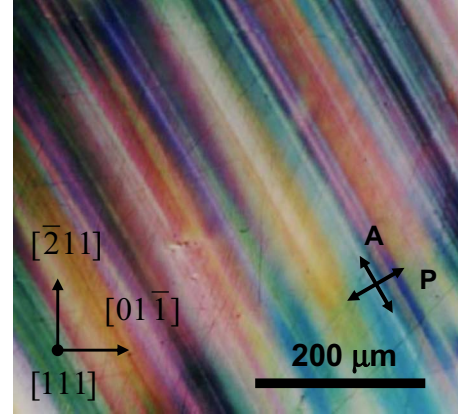


FIG. 2. (Color online) Optical domain micrograph under polarizing microscope of the (111)-oriented poled tetragonal PMN-37PT crystal plate. The crystallographic directions and the positions of crossed polarizer and analyzer are identified. Note that the observed stripes result from the interference colors, rather than from the domain walls.

point, the directions of  $P_S$  in different areas (i.e., the domain configuration) can be mapped.

To obtain the engineered domain configuration in a crystal of tetragonal symmetry, the sample should be poled by a dc electric field applied along one of the  $\langle 111 \rangle$  directions. Therefore, we prepared crystal plates with a thickness of about  $150 \mu\text{m}$  and the edges parallel to  $[111]$ ,  $[\bar{2}11]$ , and  $[01\bar{1}]$  directions, respectively (it is a convention to use the crystallographic coordinate system of the parent cubic structure to characterize the ferroelectric domain states). The largest rectangular faces corresponding to the (111) planes were mirror polished using a series of diamond pastes down to  $1 \mu\text{m}$  and the gold electrodes were deposited on these faces by sputtering. To remove the stress caused by polishing, the samples were annealed at  $500^\circ\text{C}$  for half an hour. The coercive field was estimated from ferroelectric hysteresis loops and appeared to be equal to  $6 \text{ kV/cm}$ . A much larger poling field of  $10 \text{ kV/cm}$  was used to ensure complete poling. The macroscopic piezoelectric coefficient  $d_{33}$  measured by the conventional method using a Berlincourt  $d_{33}$  meter at the frequency of  $110 \text{ Hz}$  turned out to be  $460 \text{ pm/V}$ , in agreement with the published data for the crystals of the same orientation and similar composition.<sup>24</sup> Optical domain observation and analysis were carried out by means of an Olympus BX60 polarizing microscope.

### III. RESULTS AND DISCUSSION

The spontaneous polarization  $P_S$  direction of any domain in a poled tetragonal crystal must form an angle of  $90^\circ$  with respect to the  $P_S$  of other domains. Therefore, the boundaries between domains are  $90^\circ$ -domain walls. The permissible directions of the walls can be calculated theoretically.<sup>25</sup> In the crystals of tetragonal  $4mm$  symmetry obtained by cooling from the paraelectric cubic phase of  $m\bar{3}m$  symmetry, as in the present case, the  $90^\circ$  domain walls must be parallel to one of the  $\{110\}$  crystallographic directions; all other types of

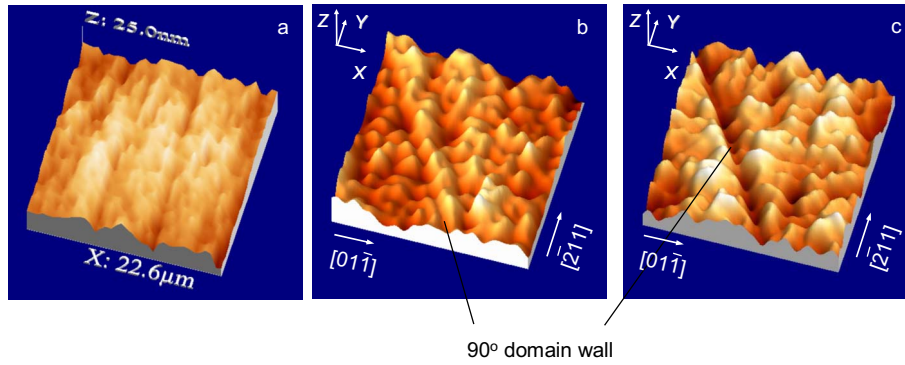


FIG. 3. (Color online) PFM images obtained on a  $23 \times 23 \mu\text{m}$  surface area of the (111)-oriented poled tetragonal PMN-37PT crystal around domain wall. (a) Surface topography. (b) and (c) Two-dimensional variations of (b) lateral and (c) vertical PFM responses.  $X$  and  $Y$  axes represent the coordinates of the measurement point in the laboratory coordinate system; PFM response is plotted on the  $Z$  axis (in arbitrary units). The domain wall is identified.

walls would have larger elastic energy. The micrograph of a poled PMN-37PT crystal viewed along the  $\langle 111 \rangle$  direction using polarizing microscope is shown in Fig. 2 (with electrodes removed). Figure 1 represents schematically the domain structure compatible with this micrograph and the theoretical predictions. Only the (101) walls are found. As a result of poling, the  $\mathbf{P}_S$  vectors in adjacent domains must be arranged in a head-to-tail configuration. As the wall bisects the angle between these vectors, it must be uncharged. Note that charged walls (with head-to-head or tail-to-tail arrangement of the  $\mathbf{P}_S$  vectors) would be perpendicular to the  $[01\bar{1}]$  direction in our crystal. However, we did not observe such a kind of walls. As the observed walls are inclined with respect to the crystal surface, the domains have the form of wedges. The wedge-shaped domains with different directions of optical indicatrix overlap each other along the way of the light propagation and the parallel fringes of interference colors appear in the micrograph. The color pattern should depend on the domain size and the number of domains through which the light propagates, which are unknown parameters. Therefore, the domain walls can hardly be distinguished. Nevertheless, the wall direction is evident: they are parallel to the color fringes and form an angle of  $60^\circ$  with respect to the  $[01\bar{1}]$  direction, which is consistent with the theoretical prediction.

In contrast to optical microscopy, the PFM studies the domain structure in the regions close to the crystal surface. Figure 3 presents the typical results of two-dimensional mapping of the same PMN-37PT crystal as shown in Fig. 2. The topography (which is obtained simultaneously with the PFM images at the same location) is shown in Fig. 3(a) (scratches from the polishing are visible). Figure 3(b) shows the lateral (measured in the  $X$  direction) piezoresponse image. There are two large areas with comparatively small and large lateral PFM response, respectively. The relative integrated intensities in these two areas are shown in Fig. 4. In Fig. 3(b), the areas are separated by the straight boundary making an angle of  $60^\circ$  with the  $X$  direction (i.e., the  $[01\bar{1}]$  crystallographic direction). Similar boundaries are observed across the sample at a distance of  $20\text{--}30 \mu\text{m}$  from one another. These boundaries are evidently the domain walls. Shear piezoelec-

tric strain (and consequently lateral PFM response) is expected to be different in different domains because of different directions of the lateral components of the  $\mathbf{P}_S$  vector ( $\mathbf{P}_{S\parallel}$ ). In contrast, the vertical  $\mathbf{P}_S$  components ( $\mathbf{P}_{S\perp}$ ) are the same and, therefore, vertical PFM response should be the same in all domains. It is, indeed, practically the same, as shown in Fig. 3(c). Nearly constant vertical response across the area is also clearly seen in Fig. 4, in which the integrated average value is shown as a function of distance from the wall. Note, however, that within  $\sim 1 \mu\text{m}$  distance of the domain wall the vertical response is significantly smaller than inside the domains. As discussed above, the vertical response is determined by the  $d_{33}$  piezoelectric coefficient. Therefore, we conclude that in the vicinity of domain wall, this piezoelectric coefficient is significantly reduced.

In the crystals which we studied the thickness of the regions with reduced piezoresponse around the walls is much smaller than the domain thickness ( $20\text{--}30 \mu\text{m}$ ) and, therefore, the influence of these regions on the average piezoelectric coefficient measured in macroscopic experiments is not expected to be dramatic. However, in poled crystals of other

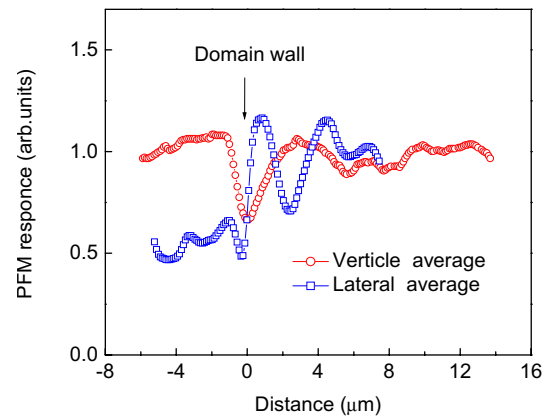


FIG. 4. (Color online) PFM response in the vicinity of  $90^\circ$  domain wall in the (111)-oriented poled tetragonal PMN-37PT crystal, represented by the variations in vertical and lateral average values integrated in the direction parallel to the wall as a function of the distance to the wall. Scales for vertical and lateral responses are different.



compositions the domain size is often much smaller and, with the decreasing domain size, this influence should increase, leading to the decrease in macroscopic piezoresponse. This is opposite to the experimental data of Wada and co-workers who observed an *increase* in  $d_{33}$  piezoelectric coefficient with the decreasing domain size in the tetragonal phase of (111)-oriented BaTiO<sub>3</sub> and KNbO<sub>3</sub>.<sup>16,17</sup>

Several hypotheses can be found in the literature concerning the influence of domain walls with engineered configuration on piezoelectric coefficients. Rao and Wang<sup>18</sup> predicted, based on computer simulations, the field-induced reversible phase transformation in the regions close to the domain wall, which should lead to an enhancement of piezoresponse. However, this enhancement is expected only in the  $\sim 5$ -nm-thick region of the wall.<sup>26</sup> If the effect is not significant enough, it may not be detected by PFM, which probes a larger region of  $\sim 30$  nm.

Dammak *et al.*<sup>11</sup> considered internal stresses that appear due to opposite piezoelectric share stress in adjacent domains when an electric field is applied. The stress may influence the longitudinal piezoelectric coefficients. However, this mechanism requires the simultaneous application of the field to both domains, like in macroscopic experiments. In the PFM measurements the field is significant only near the tip and, therefore, this effect cannot influence noticeably the PFM measurements that are performed at a distance from the wall as large as  $\sim 1$   $\mu\text{m}$ .

Hlinka *et al.*<sup>26</sup> analyzed the 90° domains in the framework of Ginzburg-Landau-Devonshire theory and found an enhancement of piezoelectric coefficients with decreasing domain thickness. However, the effect becomes significant for the domain thicknesses below  $\sim 50$  nm, i.e., much smaller than in our crystals. Besides, the piezoresponse remains constant across the wall if the realistic material parameters are used for simulations.

Damjanovic *et al.* noted that charged domain walls can enhance piezoelectric effect in the domains via the creation of depolarizing electric fields.<sup>27</sup> This effect seems to apply at least to some observations of Wada *et al.*<sup>16,17</sup> who found in many cases charged walls in their crystals. As mentioned above in this section, in our crystals the walls were uncharged. In order to further reconcile the data of Wada *et al.*

and our results, it is necessary to note that we studied the variation in piezoresponse across the single wall and had no information concerning the effect of the distance between the neighboring walls (i.e., the domain size). It is possible that the latter effect results in an increase in piezoresponse inside the domains and the overall macroscopic piezoresponse with the decrease of domain size is superior to the effect of the walls themselves.

Note that all mechanisms discussed above were proposed to justify the increase in piezoresponse due to the presence of domain walls. In our experiments we have observed the decrease of local  $d_{33}$  across the domain wall. The origin of such a surprising behavior can probably be related to the residual strains discovered around 90° walls with the help of x-ray microdiffraction experiments,<sup>28</sup> in which the strain fields were observed to extend several micrometers from the walls in the BaTiO<sub>3</sub> crystals. Although the origin of these fields remains unclear, they may change piezoelectric coefficients considerably.<sup>11,29</sup>

#### IV. CONCLUSIONS

Our results provide experimental evidence that uncharged domain walls have negative effects on the piezoelectric properties in the tetragonal relaxor PMN-PT crystals with engineered domain structure, as the  $d_{33}$  piezoelectric coefficient significantly decreases in the vicinity of the walls. To increase macroscopic  $d_{33}$  it would therefore be useful to fabricate the crystals oriented and poled along a nonpolar direction but free from uncharged walls; the method of such fabrication process needs to be developed. It would also be interesting to verify the effect of domain walls in the crystals of other compositions, in particular in the relaxor-based piezocrystals with rhombohedral structure, in which the highest piezoelectric effect has been found.

#### ACKNOWLEDGMENTS

The authors thank S. V. Kalinin and V. Yu. Topolov for helpful discussions and H. Luo for preparing the PMN-PT crystals. This work was supported by the U.S. Office of Naval Research (Grant No. N00014-06-1-0166) and the Natural Science and Engineering Research Council of Canada (NSERC).

\*Corresponding author; zye@sfu.ca

<sup>1</sup>S.-E. Park and T. R. ShROUT, J. Appl. Phys. **82**, 1804 (1997).

<sup>2</sup>R. F. Service, Science **275**, 1878 (1997).

<sup>3</sup>S.-E. Park and W. Hackenberger, Curr. Opin. Solid State Mater. Sci. **6**, 11 (2002).

<sup>4</sup>B. Noheda, Curr. Opin. Solid State Mater. Sci. **6**, 27 (2002).

<sup>5</sup>H. Fu and R. E. Cohen, Nature (London) **403**, 281 (2000).

<sup>6</sup>M. Ahrat, M. Somayazulu, R. E. Cohen, P. Ganesh, P. Dera, H. Mao, R. J. Hemley, Y. Ren, P. Liermann, and Z. Wu, Nature (London) **451**, 545 (2008).

<sup>7</sup>A. A. Bokov and Z. G. Ye, J. Mater. Sci. **41**, 31 (2006).

<sup>8</sup>R. Pirc, R. Blinc, and V. S. Vkhnin, Phys. Rev. B **69**, 212105 (2004).

<sup>9</sup>Z. Kutnjak, J. Petzelt, and R. Blinc, Nature (London) **441**, 956 (2006).

<sup>10</sup>Y. M. Jin, Y. U. Wang, A. G. Khachatryan, J. F. Li, and D. Viehland, Phys. Rev. Lett. **91**, 197601 (2003).

<sup>11</sup>H. Dammak, A.-E. Renault, P. Gaucher, M. P. Thi, and G. Calvarin, Jpn. J. Appl. Phys., Part 2 **42**, 6477 (2003).

<sup>12</sup>V. Yu. Topolov, J. Phys.: Condens. Matter **16**, 2115 (2004).

<sup>13</sup>G. Xu, J. Wen, C. Stock, and P. M. Gehring, Nature Mater. **7**, 562 (2008).

<sup>14</sup>J. Y. Li, R. C. Rogan, E. Ustundag, and K. Bhattacharya, Nature Mater. **4**, 776 (2005).

<sup>15</sup>D. Damjanovic, Rep. Prog. Phys. **61**, 1267 (1998).

<sup>16</sup>S. Wada, S. Suzuki, T. Noma, M. Osada, M. Kakihana, S.-E.

- Park, L. E. Cross, and T. R. ShROUT, Jpn. J. Appl. Phys., Part 2 **38**, 5505 (1999).
- <sup>17</sup>S. Wada, T. Muraishi, K. Yokoh, K. Yako, H. Kamemoto, and T. Tsurumi, *Ferroelectrics* **355**, 37 (2007).
- <sup>18</sup>W.-F. Rao and Y. U. Wang, *Appl. Phys. Lett.* **90**, 041915 (2007).
- <sup>19</sup>A. Gruverman and S. V. Kalinin, *J. Mater. Sci.* **41**, 107 (2006).
- <sup>20</sup>Z.-G. Ye and M. Dong, *J. Appl. Phys.* **87**, 2312 (2000).
- <sup>21</sup>I. K. Bdikin, V. V. Shvartsman, S. H. Kim, J. M. Herrero, and A. L. Kholkin, in *Ferroelectric Thin Films XII*, edited by S. Hoffmann-Eifert *et al.*, MRS Symposia Proceedings No. 784 (Material Research Society, Pittsburgh, 2003), p. C11.3.
- <sup>22</sup>I. Horcas, R. Fernández, J. M. Gómez-Rodríguez, J. Colchero, J. Gómez-Herrero, and A. M. Baro, *Rev. Sci. Instrum.* **78**, 013705 (2007).
- <sup>23</sup>B. J. Rodriguez, A. Gruverman, A. I. Kingon, R. J. Nemanich, and J. S. Cross, *J. Appl. Phys.* **95**, 1958 (2004).
- <sup>24</sup>Z. Feng, X. Zhao, and H. Luo, *J. Phys.: Condens. Matter* **16**, 6771 (2004).
- <sup>25</sup>J. Erhart, *Phase Transitions* **77**, 989 (2004).
- <sup>26</sup>J. Hlinka, P. Ondrejko, and P. Marton, *Nanotechnology* **20**, 105709 (2009).
- <sup>27</sup>D. Damjanovic, M. Davis, and M. Budimir, in *Handbook of Advanced Dielectric, Piezoelectric and Ferroelectric Materials: Synthesis, Properties and Applications*, edited by Z.-G. Ye (Woodhead, Cambridge, 2008), Chap. 11, p. 322.
- <sup>28</sup>R. C. Rogan, N. Tamura, G. A. Swift, and E. Ustundag, *Nature Mater.* **2**, 379 (2003).
- <sup>29</sup>M. Budimir, D. Damjanovic, and N. Setter, *Phys. Rev. B* **73**, 174106 (2006).